MODIFICATION OF EEG BRAIN ACTIVITY INDUCED BY RESPIRATORY MUSCLE REGULATION DURING PHONATION

Said-Iraj Hashemi [1, 2], Mathieu Petieau [1], Guy Cheron [1], Didier Demolin [2], Ana Maria Cebolla [1]

[1]Laboratory of Neurophysiology and Movement Biomechanics (LNMB). Faculty of Motor Skills Sciences | Motricity Sciences Research Center. Interfaculty institutes | UNI, ULB Neuroscience Institute Université Libre de Bruxelles, Brussels, Belgium.
[2]Phonetics and Phonology Laboratory LPP, CNRS-UMR 7018, Sorbonne Nouvelle, Paris, France

Abstract

This paper presents the results of an experiment replicating Ladefoged's (1967) experiment of variations in subglottal pressure and respiratory muscles activity during speech. We set up a methodology in which acoustic and aerodynamic parameters, respiratory muscles, and the electroencephalogram (EEG) activity are for the first time synchronously, registered with one participant producing a suite of [pa] in one long expiration. 4 phases in the regulation of subglottal pressure were identified: (1) the elastic recoil of the inspiratory muscles, (2) the activity the internal intercostals, (3) and (4) the abdominal muscles activations. Interestingly brain oscillations showed identifiable power spectrum modulations of alpha and theta brain rhythms specifically related to the four phases, suggesting specific brain function accompanying expiration phases. The latency of these phases corroborates with the different patterns of EEG activity during the sequences of [pa] syllable production.

1. INTRODUCTION

During the production of speech, there is an increase in the average level of the subglottic pressure (Ps). This pressure returns to its baseline level after the end of the utterance. Slight variations in the average Ps can be observed during a long utterance. In his work published in the book "three areas of experimental phonetics", published in 1967[1], Peter Ladefoged highlighted the different actions of the respiratory muscles responsible for maintaining the Ps during a long utterance. After a deep inspiration, the relaxation pressure is much higher than the required pressure under the vocal folds, the inspiratory muscles relax and pressure decreases in the lungs. When the relaxation (the recoil forces) becomes low, the inspiratory muscles usually stop working and the pressure required for speech is maintained by the work of the expiratory muscles. Toward the end of a long utterance, when the volume of air in the lungs is very low, many expiratory muscles may be needed to maintain pressure at a constant level.

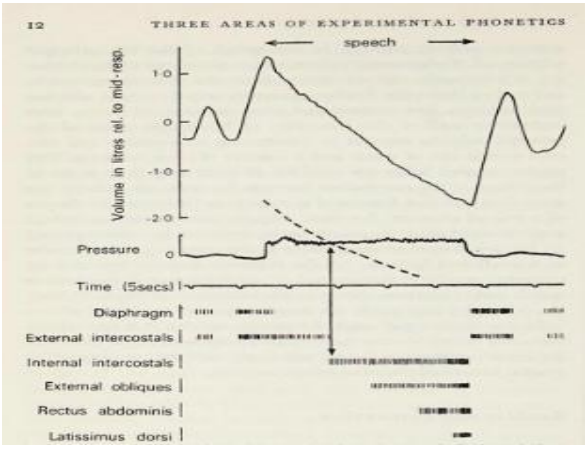

Figure 1. Ladefoged experiment, relating aerodynamic and myologic parameters during a long statement (the subject counted from 1 to 32 without taking a breath)

The lower part of figure 1 illustrates schematically the activity of the respiratory muscles to maintain a constant average pressure. The action of the external intercostals ceases when the volume of air in the lungs is slightly lower than the volume after a normal inspiration. From this point on, expiratory activity is necessary to maintain the pressure under the vocal folds and, therefore, the internal intercostals come into action with progressively increasing intensity. The action of the internal intercostals is complemented by various other muscles, such as the external obliques, rectus abdominis and dorsalis major. These muscle actions could be modulated by the oscillatory activity of the neocortex.

EEG oscillations are direct global electrical brain activity underlying brain function [2] EEG dynamics can be characterized by time-frequency domain measures such as the power spectrum [3] and phase variations of EEG oscillations [4]. For example, in a relaxed awake state, when the eyes are closed, the power of the EEG alpha rhythm (8-13 Hz) increases in the occipital and parietal scalp areas [5]. The increase in alpha power is related to the maintenance of neural network coherence in the absence of visual and sensorimotor information and is considered a marker of cortical inactivity or an indication of active inhibition of sensory information [6]. The increase in the power spectrum (ERS) of theta oscillation in the motor area plays an important function in motor control. In addition, theta oscillation is thought to be phase-locked with movement onset, and theta power is correlated with movement acceleration [7].

The role of brain activity in controlling the mechanisms responsible for phonation remains unknown. Among the rares studies, Lizarazu and all were interested in the adaptation of brain oscillations

to speech rate. Assuming that the delta (<4 Hz) and theta (4-8 Hz) frequency bands drive prosodic and syllabic speech rates respectively. And that the theta band modulates high-frequency neural oscillations in the gamma band (25-40 Hz), which are thought to be crucial for phoneme processing in natural speech, they asked subjects to deliver speech at slowed, normal, and accelerated rates. Their results show that the phase of theta band oscillations in auditory regions adjusts to variations in speech rate. Moreover, they have demonstrated a phase-amplitude coupling between the gamma and theta frequency bands respectively, which follows the speech rate[8].

Another team was interested in the neural mechanisms underlying the coordination and articulation of movements during speech[9]. Participants read aloud 460 sentences from the MOCHA-TIMIT[10] database. The authors focused primarily on the sensorimotor cortex and inferred the articulator movements of the speakers from the acoustics of the speech produced. The main results of their work show that articulatory kinematic trajectories reveal coordinated movements of the tongue, lips, jaw, and larynx and are encoded by the sensorimotor cortex. Finally, we can mention Galgano and colleagues[11] who studied brain generators of voice-related cortical potentials (VRCPs). Participants held their breath for 4 seconds and, after the appearance of a visual signal, they emitted the sound [m] while keeping their mouths closed or exhaled through their nose without emitting a sound. Examination of the spatiotemporal changes in the VRCP -150ms before the onset of phonation and 100ms after the onset of phonation, revealed the involvement of the laryngeal motor cortex, probably responsible for the execution and continuity of phonation. Other sources were also located in the cerebellum.

To our knowledge there is no published study of cortical patterns associated with Ps regulation and the underlying muscle actions during a long utterance. According to Ladefoged's work, during the production of short utterances, Ps regulation occurs autonomously and with the help of recoil forces. However, in the case of a long utterance, this is regulated with the help of the action of the expiratory muscles. In this preliminary work, we revisited the study of Ladefoged 1967, and studied the oscillatory brain patterns underlying the different phases of phonation during expiration and their transition.

2.METHOD

2.1 Subject and protocol

This study was approved by the ethics committee of the Brugmann University Hospital (EC 2022/246). Our participant was a 63-year-old French-speaking male. We replicated the experience of Ladefoged in its "three areas of experimental phonetics" study with a modified statement. Indeed, the protocol consisted in producing the syllable [pa] as long as possible without taking a breath. The participant sat in a chair, took a normal breath, and began to pronounce the syllable [pa] at a self-regulated rate. We recorded 15 sequences of [pa] syllable production.

2.2 Materials

Acoustic parameters were recorded using the Assisted Vocal Assessment System (EVA2) with a sampling frequency of 4400 Hz. We determined the Ps from the intraoral pressure, we also measured the vibration of the vocal folds.
Respiratory muscle activity was recorded with bipolar Delsys EMG TrignoTM surface electrodes on the scalene, external, and internal intercostal, external oblique, and rectus abdominis muscles, with a sampling frequency of 2000 Hz.
EEG signals during [pa] sequences were recorded using the ANT system (sampling rate 2048 Hz), (Netherlands) Neuro with a 128-channel EEG cap comfortably fitted to the participant's head. Electrodes located on both mastoids served as EEG reference. All recording systems were synchronized with each other using an external signal generator sending triggers at the beginning and end of each recording.

3. AERODYNAMIC, EMG, EEG ANALYSIS

3.1 Aerodynamic and EMG analysis

We used the Winpitch LTL software (Martin 2004) to analyze the acoustic parameters of the [pa] syllable production sequences. A visual analysis of the evolution of the estimated Ps allowed us to highlight slight fluctuations during the sequence [pa]. These fluctuations are concomitant with the action of the respiratory muscles. As shown in figure 2, the successive actions of the muscles constitute the different phases of the regulation of the Ps. The elastic recoil of the diaphragm and external intercostal, constitutes phase 1 (P0 and P1). The internal intercostal action constitutes phase 2 (P2). The external oblique action is associated with phase 3 (P3). And finally, the action of the rectus abdominis (P4), at the end of the sequence [pa], constitutes the

last phase of regulation of the Ps.

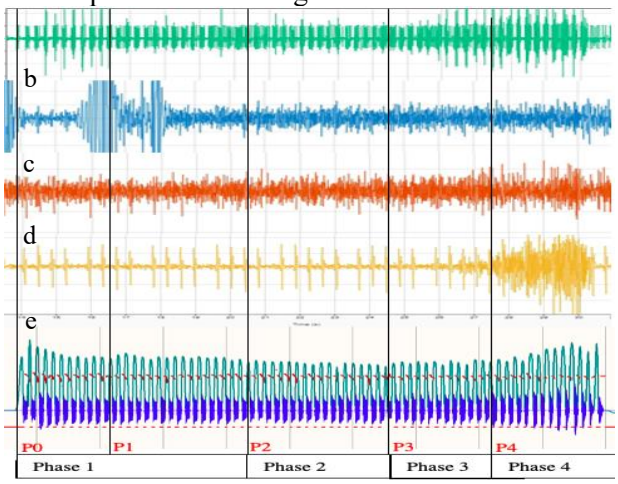

Figure 2 Variation of myologic and aerodynamic parameters during a [pa] sequence. a: Scalene; b: external intercostal; c: external oblique; d: rectus abdominis; e: green curve estimated of the measured Ps; blue curve: vocal folds vibration; red lines: fundamental frequency

3.2 EEG analysis

EEG data was processed using The Math Works, lnc. MATLAB version 2022a and an open-source toolbox EEGLAB v2022.1, Delorme A & Makeig S (2004). After a visual identification and removal of noisy channels, we filtered the data with a 0.5 Hz high-pass filter. The line noise was removed using Zapline plugin [12]. We then performed an independent component analysis (ICA). Components associated with eye movements, heartbeat, channel noise and muscle activity were identified by visual analysis and using ICLabel plugin and were rejected. Only components with at least a 10% probability of containing brain activity were retained. The events related to every phase latency were imported. We spliced the data according to the [pa] sequences and performed time-frequency analyses in the frequency band 1 to 30 Hz on channels F3, C3 and P3 (frontal, central and parietal sites situated on the left at the scalp level). The average duration of the [pa] sequences was 20± 2s. The baseline was therefore defined 2 seconds before the sequences.

4. RESULTS

4.1 Descriptive statistics

The average duration of P1 is 7.54 ± 2.2 s (composed of P0 3.97 ± 1.26s and P1 3.57 ± 0.94), P2 3.94 ± 1.33s, P3 4.11± 1.40s and P4 with 3.64 ± 0.84s. Regarding the duration of scalene muscle contraction during the production of the syllable [pa], a progressive increase was observed. With the minimum time in P1 0.105 ± 0.030ms and the maximum time in P4 0.149 ± 0;054ms.

4.3 Time-frequency analysis

For time-frequency analysis of EEG oscillations, we calculated the baseline normalized spectrogram or ERSP (2s before the P0 event) [3,4]. Event-related spectral perturbation (ERSP) measures variations in the power spectrum of ongoing rhythms at specific time periods and frequency ranges. In ERSP measurements, ERD (event related desynchronization) indicates a reduction in the power spectrum while ERS (event related synchronization) indicates an increase in the power spectrum. ERD/ERS are interpreted as reflecting the reactivity of the brain and are related to specific aspects of information processing in the brain. We also calculated the ITC [13] which measures the phase coherence between ongoing EEG signals at specific time periods and frequency ranges. For the significance level of ERSP and ITC, a bootstrap resampling ($p < 0.05$) was used as a surrogate method.

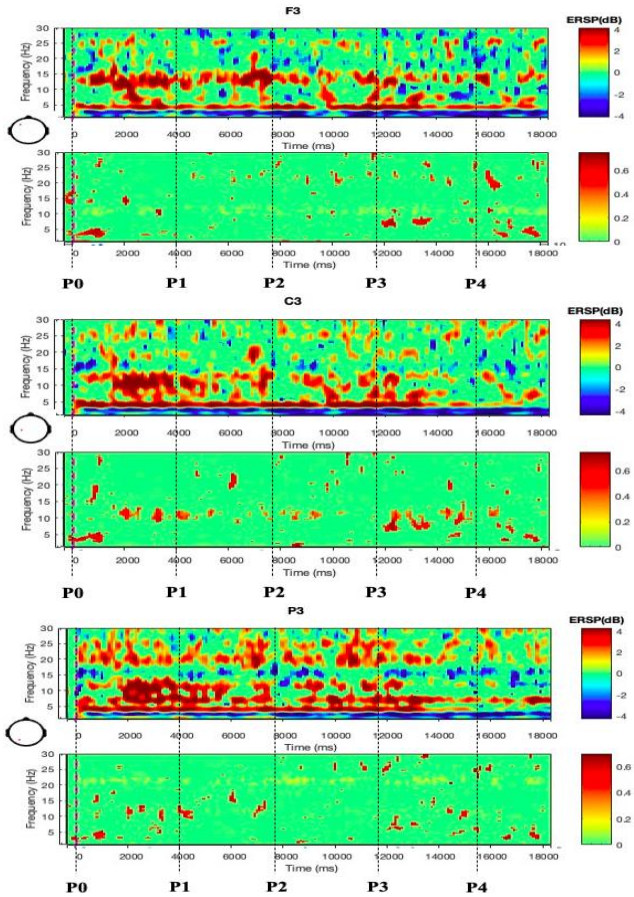

Figure 3 Time-frequency analysis of time-locked [pa] sequences.

Figure 3 shows the average ERSP of time-locked [pa] sequences. The average ERSP spectrogram of F3 shows a clear increase in the power spectrum (event-related synchronization, ERS) at the maxima of 13 Hz and at 7 Hz (ranging from about 4 to 14 Hz) from P0 to P1. Then a large ERS in the 4 Hz to 14 Hz frequency band at 2500ms after P0 and at the end of P1 and P2 is observed. A decrease in spectral

power (ERD) centered at 7 Hz is observed at the end of P3, being followed by an ERS centered at 13 Hz at the beginning of P4. The ERSP on electrode C3, shows similar dynamics as F3, with the particularity of a lower theta ERD at the end of P3 and a lower Alpha ERS at the beginning of P4.
The ERSP of the P3 electrode shows a continuous increase in spectral power (ERS) at 4 Hz until the end of phase 3. And a discontinuous increase in spectral power at 7 Hz at 1800ms until the end of the sequence. We note a ERS centered at 15 Hz in a jerky manner at 0ms and around the latency of each phase. We observe an absence of alpha spectral power from 12600ms, and an ERD in the alpha band at the end of the sequence. Interestingly, variations of theta oscillations accompany variations of alpha oscillations, suggesting the constitution of a unified theta-alpha pattern.
The ITC patterns of F3, C3, and P3 (Figure 3) showed a phase synchronization cluster centered at 4 Hz during the first 1000ms of the sequence. There is a 7-Hz synchronization cluster at 12000 and 13000ms and a 4-Hz synchronization cluster at 17000 and 18000ms in the F3, C3, and P3 electrodes. Finally, we observe a 12 Hz synchronization cluster at 2000 and 3000ms in electrodes C3 and P3.

4.4 Topographical analysis of the ERSP

The topography (128 EEG electrodes) of the ERSP (Figure 4) in the theta frequency band (4-7 Hz) shows an ERS in the central, parietal, and occipital regions at P0. The increase in ERS is centered in the parietal and occipital regions at the end of phase 1. We then observe an increase in ERS, centered in the left lateral and parietal regions, before and during P3 and at the beginning of phase 4. At the end of the sequence, we observe ERS, only in the parietal region at 16s. At 17s, we observe generalized ERS only on the left side of the scalp. Theta spectral power continues to decrease from 18s.

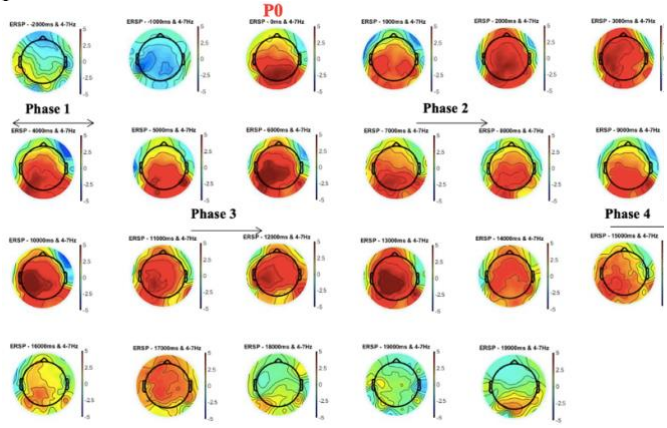

Figure 4 Topography analysis of ERSP sequences of [pa] locked in time. In the Theta frequency band

The topography of the ERSP (Figure 5) in the Alpha frequency band (8 to 13 Hz) shows a localized ERS in the left lateral region at the beginning of phase 1, at 1000ms. We then observe an increase in ERS in all regions of the scalp. At the end of phase 1, we again see a localized ERS increase in the left lateral region. At the intersection of phases 2 and 3, we again observe an increase in spectral power in the left lateral region. Interestingly, the ERSP topography in the theta band showed an ERS in the same region and at the same time. At the beginning of phase 4, there is an ERS in the occipital region and ERD at the end of this phase (at 19s) throughout the scalp and especially in the occipital region.

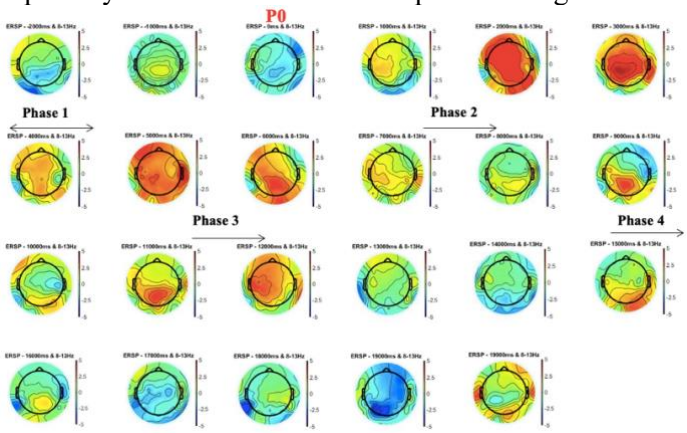

Figure 5 Topography analysis of ERSP sequences of [pa] locked in time. In the Alpha frequency band

5.DISCUSSION

We replicated Ladefoged's (1967) experiment on variations in Ps and respiratory muscle activity during speech. By calculating the ERSP in the time-frequency domain (figure 3) and the topography of the ERSP in the theta and alpha frequency bands (figure 4 and 5), we showed that there are patterns of variation in the spectral power (ERS and ERD) of these frequency bands that underly the phases of the regulation of the Ps. Moreover, the variation of the spectral power of the alpha frequency band is concomitant to the spectral variation of theta band, in the vicinity of the phase transitions.
The strong point of our methodology compared to the study of Louks [14] is the synchronization of the EEG , the electromyography, aerodynamic and the acoustics signals. A more in-depth study of source analysis will allow to investigate the precise regions of the neocortex areas involved in the regulation of Ps seems essential to us. Furthermore, we question the contribution of the cerebral cortex in the transition from autonomous to controlled regulation.

This study is funded by the French National Research Agency (ANR) within the framework of the full 3D talking head project.

6. REFERENCES

[1] Ladefoged P. Three areas of experimental phonetics : stress and respriatory activity, the nature of vowel quality, units in the perception and production of speech. --. London : Oxford U.P.; 1967.
[2] Buzsáki G, Draguhn A. Neuronal oscillations in cortical networks. Science 2004;304:1926–9. https://doi.org/10.1126/science.1099745.
[3] Pfurtscheller G, Stancák A, Neuper Ch. Event-related synchronization (ERS) in the alpha band — an electrophysiological correlate of cortical idling: A review. International Journal of Psychophysiology 1996;24:39–46. https://doi.org/10.1016/S0167-8760(96)00066-9.
[4] Makeig S, Debener S, Onton J, Delorme A. Mining event-related brain dynamics. Trends in Cognitive Sciences 2004;8:204–10. https://doi.org/10.1016/j.tics.2004.03.008.
[5] Tudor M, Tudor L, Tudor KI. [Hans Berger (1873-1941)--the history of electroencephalography]. Acta Med Croatica 2005;59:307–13.
[6] Pfurtscheller G, Neuper C, Mohl W. Event-related desynchronization (ERD) during visual processing. International Journal of Psychophysiology 1994;16:147–53. https://doi.org/10.1016/0167-8760(89)90041-X.
[7] Ofori E, Coombes SA, Vaillancourt DE. 3D Cortical electrophysiology of ballistic upper limb movement in humans. NeuroImage 2015;115:30–41. https://doi.org/10.1016/j.neuroimage.2015.04.043.
[8] Lizarazu M, Lallier M, Molinaro N. Phase−amplitude coupling between theta and gamma oscillations adapts to speech rate. Annals of the New York Academy of Sciences 2019;1453:140–52. https://doi.org/10.1111/nyas.14099.
[9] Chartier J, Anumanchipalli GK, Johnson K, Chang EF. Encoding of Articulatory Kinematic Trajectories in Human Speech Sensorimotor Cortex. Neuron 2018;98:1042-1054.e4. https://doi.org/10.1016/j.neuron.2018.04.031.
[10] MOCHA-TIMIT n.d. https://www.cstr.ed.ac.uk/research/projects/artic/mocha.html (accessed April 28, 2023).
[11] Galgano J, Froud K. Evidence of the voice-related cortical potential: an electroencephalographic study. Neuroimage 2008;41:1313–23. https://doi.org/10.1016/j.neuroimage.2008.03.019.
[12] Klug M, Kloosterman NA. Zapline-plus: A Zapline extension for automatic and adaptive removal of frequency-specific noise artifacts in M/EEG. Hum Brain Mapp 2022;43:2743–58. https://doi.org/10.1002/hbm.25832.
[13] Tallon-Baudry C, Bertrand O, Delpuech C, Pernier J. Stimulus Specificity of Phase-Locked and Non-Phase-Locked 40 Hz Visual Responses in Human. J Neurosci 1996;16:4240–9. https://doi.org/10.1523/JNEUROSCI.16-13-04240.1996.
[14] Loucks TMJ, Poletto CJ, Simonyan K, Reynolds CL, Ludlow CL. Human brain activation during phonation and exhalation: Common volitional control for two upper airway functions. NeuroImage 2007;36:131–43. https://doi.org/10.1016/j.neuroimage.2007.01.049.